Electronic Supplementary Material (ESI) for RSC Advances.

Supplementary Information

Solution-Processed MoS_2 Nanotubes/Reduce Graphene Oxide Nanocomposite as an Active Electrocatalyst toward Hydrogen Evolution Reaction

Supplementary Figures and Tables.

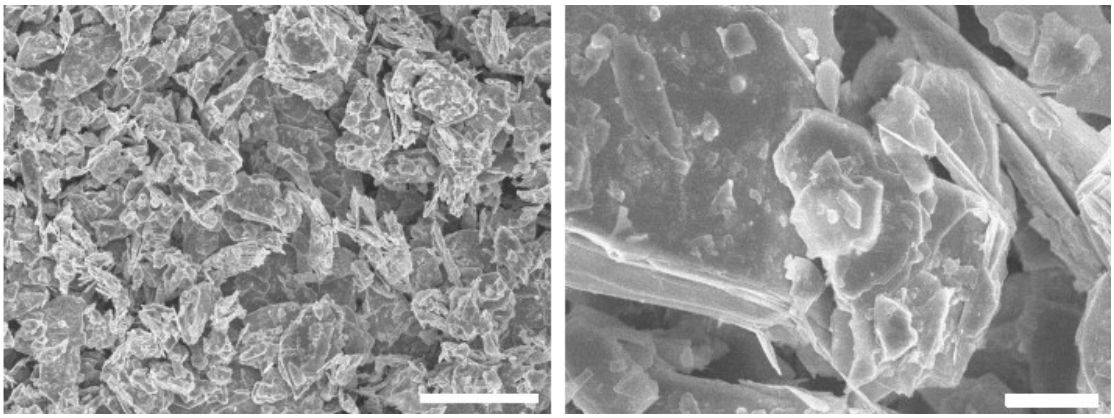

Fig. S1. SEM images of typical commercial Bulk MoS_2 (BM). The scale bars are 10 μm and 1 μm, respectively.

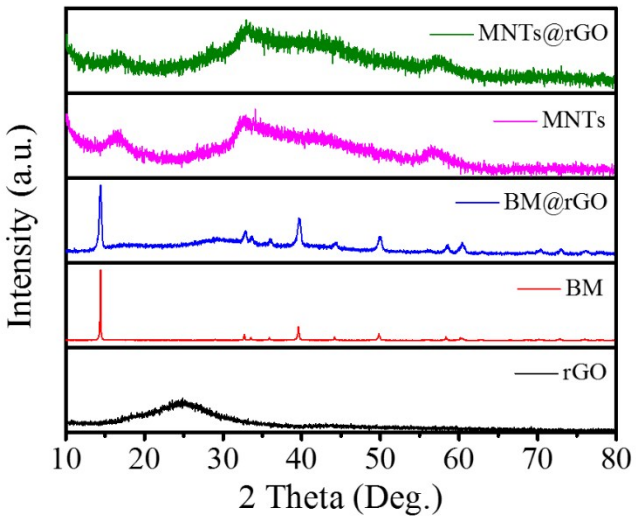

1

2 Fig. S2. XRD patterns of rGO, BM, BM@rGO, MNTs and MNTs@rGO.

3

For MNTs@rGO hybrids, all the characteristic diffraction peaks of MNTs can be observed, while the absence of peaks at low-angle region indicates that the MoS_2 nanosheets are not restacked, which is beneficial for the exposure of electrocatalytic active sites. Moreover, the absence of diffraction peaks for rGO in the composites may be ascribed to the relative low content of rGO and the relatively higher intensity of the diffraction peaks for MNTs.

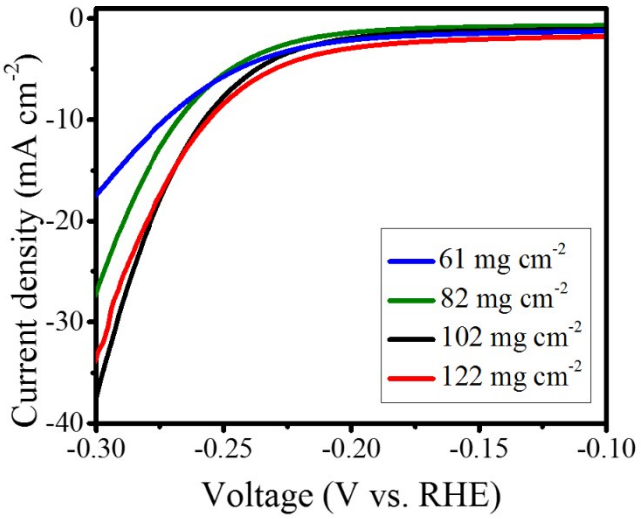

Fig. S3. The polarization curves of MNTs@rGO at different loading weight.

Table S1. Comparison of the electrocatalytic activity of MNTs@rGO to some representative MoS_2-based HER catalysts reported in the literature.

Sample	Onset Potential (mV vs. RHE)	Tafel Slope (mV dec^{-1})	η (mV vs. RHE) for J = -10 mA cm^{-2}	Catalyst loading (μg cm^{-2})	Ref.
MoS_2 composite (nanosheets & quantum dots)	-120	69	~ 250	35.7	S1
2D MoS_2 nanosheets	-80	90	~ 210	571	S2
Pd coated MoS_2 nanoflowers	-218	39	-	3538	S3
MoS_2 nanoflowers@rGO	-190	95	285	-	S4
Defect-rich MoS_2	-120	50	180	285	S5
Nanoporous MoS_2	~ -150	50	270	60	S6
MoS_3 nanoparticles	-150	41-63	260	32	S7
MoO_3-MoS_2 core-shell nanowires	-150	50-60	250	60	S8
MoS_2@carbon paper	-200	120	-	-	S9
Supported $[Mo_3S_4]^{4+}$	-200	120	280	-	S10
Graphene nanoribbon-supported MoS_2 nanosheets	-110	43.4	180	285	S11
S-doped carbon modified MoS_2 nanosheets	-60	72	~ 180	-	S12
MoS_2 quantum dots interspersed in MoS_2 sheets	-190	74	-	-	S13
MNTs@rGO	-180	69	250	102	This work

Double layer capacitance (C_{dl}) calculations.

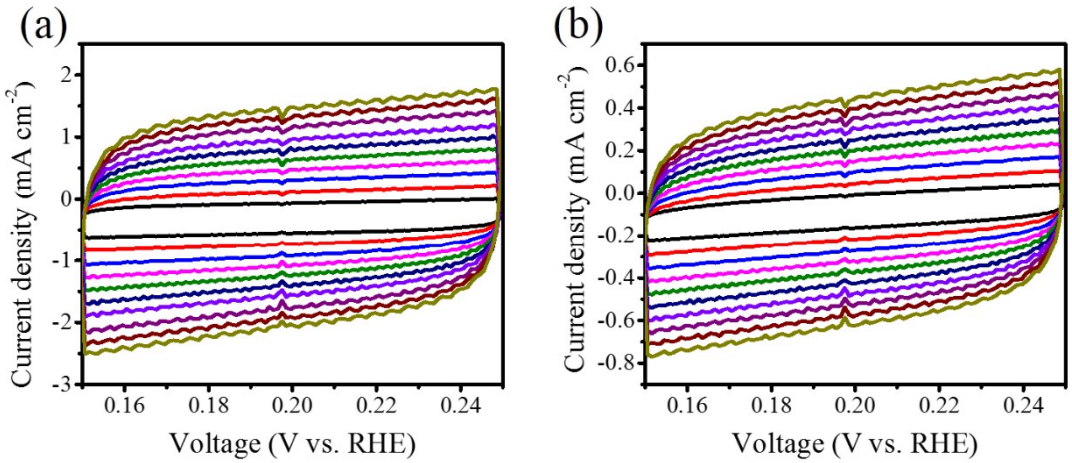

Fig. S4. CV curves of MNTs@rGO (a) and BM@rGO (b) at different scan rates in the potential region of 0.15−0.25 V vs. RHE, respectively.

To estimate the effective active surface area of the MNTs@rGO and BM@rGO, the CV curves were performed at a series of scan rates (20, 40, 60, 80, 100, 120, 140, 160, 180 and 200 mV s^{-1}) in the potential range of 0.15−0.25 V vs. RHE, which was considered as the double layer capacitance (C_{dl}) behavior. The C_{dl} values of MNTs@rGO and BM@rGO were estimated by plotting the ΔJ (J_{anodic}-$J_{cathodic}$) at 0.2 V *vs*. RHE against the scan rate, where the slope of the resulting curve was twice of the C_{dl} (Fig. 4e).[S11]

Turnover frequency (TOF) calculations.

The TOF value is calculated from the equation: [S15]

$$\mathrm{TOF} = (J^{*}A) / (2^{*}F^{*}n)$$

where J is the current density at a given overpotential, A is the surface area of the electrode, the number 2 means two electrons are required to form one hydrogen molecule from two protons, F is the Faraday constant and M is the number of moles of sulfide atoms on the electrode. It must be noted that this TOF estimate assumes that all of the S atoms present in the material are catalytically active. However, only the edges of the MoS_2 are identified as the active sites for the HER reactions, where the unsaturated S atoms are exposed and can absorb protons with a small free energy.[S16] The vast majority of the S atoms in the nanotubes are expected to play a purely structural role, which results in a gross overestimate of the real number of active sites. Thus, we can conclude that the calculated TOFs only represented the lower limit.

Table S2. Fit parameters of EIS spectra measured at different η values for MNTs@rGO modified electrode

η (mV)	R_{ct} (Ω)	R_m (Ω)	C_{int} (F)	τ_{ct} ($\Omega^{1/2}$ $F^{1/2}$)	τ_m ($\Omega^{1/2}$ $F^{1/2}$)
150	273.3	6.311	0.00697	1.90534	0.044
160	182	6.168	0.00691	1.25758	0.04262
170	125.6	5.871	0.00684	0.85861	0.04013
180	88.19	5.541	0.00676	0.59616	0.03746
190	62.11	5.297	0.0067	0.41632	0.03551
200	44.6	4.843	0.00667	0.29733	0.03229
210	32.74	4.682	0.00656	0.21484	0.03072
220	24.48	4.415	0.00649	0.15888	0.02866
230	18.85	4.18	0.0064	0.12057	0.02674
240	14.35	3.917	0.00644	0.09235	0.02521
250	11.14	3.757	0.0064	0.07126	0.02403
260	8.99	3.41	0.00659	0.05922	0.02246

Table S3. Fit parameters of EIS spectra measured at different η values for BM@rGO modified electrode

η (mV)	R_{ct} (Ω)	R_m (Ω)	C_{int} (F)	τ_{ct} ($\Omega^{1/2}$ $F^{1/2}$)	τ_m ($\Omega^{1/2}$ $F^{1/2}$)
230	3269	7.907	0.00125	4.0771	0.00986
240	3054	7.999	0.00121	3.70145	0.00969
250	1860	7.721	0.00128	2.37522	0.00986
260	2358	8.008	0.00119	2.79871	0.0095
270	1845	8.042	0.00117	2.16123	0.00942
280	1696	8.205	0.00114	1.93853	0.00938
290	1496	8.274	0.00113	1.6836	0.00931
300	1385	8.465	0.0011	1.52392	0.00931
310	1234	9.015	0.00105	1.32556	0.00945
320	1219	9.533	0.00101	1.22826	0.00961
330	1155	10.09	0.00097	1.12235	0.0098
340	975.4	10.9	0.00093	0.90849	0.01015

References to Supplementary Information

S1. S. Xu, D. Li and P. Wu, *Adv. Funct. Mater.*, 2015, **25**, 1127.

S2. S. Muralikrishna, K. Manjunath, D. Samrat, V. Reddy, T. Ramakrishnappa and D.H. Nagaraju, *RSC Adv.*, 2015, **5**, 89389.

S3. B. B. Li, S. Z. Qiao, X. R. Zheng, X. J. Yang, Z. D. Cui, S. L. Zhu, Z. Y. Li and Y. Q. Liang, *J. Power Sources*, 2015, **284**, 68.

S4. C. B. Ma, X. Qi, B. Chen, S. Bao, Z. Yin, X. J. Wu, Z. Luo, J. Wei, H. L. Zhang and H. Zhang, *Nanoscale*, 2014, **6**, 5624.

S5. J. Xie, H. Zhang, S. Li, R. Wang, X. Sun, M. Zhou, J. Zhou, X. W. (David) Lou and Y. Xie, *Adv. Mater.*, 2013, **25**, 5807.

S6. J. Kibsgaard, Z. Chen, B. N. Reinecke and T. F. Jaramillo, *Nature Mater.*, 2012, **11**, 963.

S7. H. Vrubel, D. Merki and X. Hu, *Energy Environ. Sci.*, 2012, **5**, 6136.

S8. Z. Chen, D. Cummins, B. N. Reinecke, E. Clark, M. K. Sunkara and T. F. Jaramillo, *Nano Lett.*, 2011, **11**, 4168.

S9. J. Bonde, P. G. Moses, T. F. Jaramillo, J. K. Nørskov and I. Chorkendorff, *Faraday Discuss.*, 2008, **140**, 219.

S10. T. F. Jaramillo, J. Bonde, J. Zhang, B. L. Ooi, K. Andersson, J. Ulstrup and I. Chorkendorff, *J. Phys. Chem. C*, 2008, **112**, 17492.

S11. Y. Zhao, F. Zhao, X. Wang, C. Xu, Z. Zhang, G. Shi and L. Qu, *Angew. Chem. Int. Ed.*, 2014, **53**, 13934.

S12. H. Gu, L. Zhang, Y. Huang, Y. Zhang, W. Fan and T. Liu. *RSC Adv*., 2016, **6**, 13757.

S13. T.N. Kumar, N. Chandrasekaran and K. L. Phani, *Chem. Commun.*, 2015, **51**, 5052.

S14. D. Gopalakrishnan, D. Damien and M. M. Shaijumon, *ACS Nano*, 2014, **8**, 5297.

S15. D. Merki, H. Vrubel, L. Rovelli, S. Fierro and X. Hu, Chem. Sci., 2012, **3**, 2515.

S16. Y. Yan, B. Xia, Z. Xu, X. Wang, *ACS. Catal.*, 2014, **4**, 1693.